J. Fluid Mech. (1978), *vol.* 85, *part* 3, *pp.* 573–589
Printed in Great Britain

The 'Hurst phenomenon' in grid turbulence

By K. N. HELLAND AND C. W. VAN ATTA
Department of Applied Mechanics and Engineering Sciences,
University of California, La Jolla

(Received 30 June 1976 and in revised form 6 January 1977)

Measurements of the statistical property called the 'rescaled range' in grid-generated turbulence exhibit a Hurst coefficient $H = 0{\cdot}5$ for $43 < UT/M < 1850$, where M/U is a characteristic time scale associated with the grid size M and mean velocity U. Theory predicts that $H = 0{\cdot}5$ for independence of two observations separated by a time interval T, and the deviation from $H = 0{\cdot}5$ is referred to as the 'Hurst phenomenon'. The rescaled range obtained for grid turbulence contains an initial region $UT/M < 43$ of large H, approaching $1{\cdot}0$, corresponding approximately to the usual region of a finite non-zero autocorrelation of turbulent velocity fluctuations. For $UT/M > 1850$ the rescaled range breaks from $H = 0{\cdot}5$ and rises at a significantly faster rate, $H = 0{\cdot}7$–$0{\cdot}8$, implying a long-term dependence or possibly non-stationarity at long times. The measured autocorrelations remain indistinguishable from zero for $UT/M > 20$. The break in the trend $H = 0{\cdot}5$ is probably caused by motions on scales comparable to characteristic time scales of the wind-tunnel circulation. Rescaled-range analysis is a powerful statistical tool for determining the time scale separating the grid turbulence from the background wind-tunnel motions.

1. Introduction

The rescaled range R/S of the time series $y(t)$, using the notation of Nordin, McQuivey & Mejia (1972), is defined by

$$R/S = R(t, T)/S(t, T), \tag{1}$$

where

$$R(t, T) = \max_{0 \leqslant t' \leqslant T}\left[\int_0^{t'} y(t)\,dt - \frac{t'}{T}\int_0^T y(t)\,dt\right] - \min_{0 \leqslant t' \leqslant T}\left[\int_0^{t'} y(t)\,dt - \frac{t'}{T}\int_0^T y(t)\,dt\right], \tag{2}$$

$$S^2(t, T) = \operatorname{var} y(t) = \frac{1}{T}\int_0^T \left[y(t) - \frac{1}{T}\int_0^T y(t)\,dt\right]^2 dt. \tag{3}$$

The Hurst coefficient H is obtained by measuring the slope of the curve obtained by plotting the rescaled range R/S *vs.* T on logarithmic axes.

In 1951 Hurst introduced the rescaled range R/S as a measure of long-term persistence in geophysical time series. It has been shown theoretically by Feller (1951) and Anis & Lloyd (1953) that $R/S \sim T^{0{\cdot}5}$ for large T. This theoretical result contradicts the almost universal empirical results, which give $R/S \sim T^H$ with $0{\cdot}5 < H < 1{\cdot}0$. For example, Hurst (1951) reports coefficients of about $0{\cdot}7$–$0{\cdot}85$ for the Nile River annual outflow and for other time series of natural phenomena such as the size of tree rings and varves (sediment deposits). The failure of classical theories of stationary stochastic processes to provide examples of the Hurst phenomenon to supplement empirical evidence is summarized by Lloyd (1967). However, Mandelbrot (1965) and Mandelbrot & Van Ness (1968) point out that $H \neq 0{\cdot}5$ occurs in a class of stochastic processes they call fractional Brownian noises, which contain an infinite domain of dependence, or infinite memory. Mandelbrot (1965) suggests that fractional Brownian noise processes can be used as operational models for hydrological problems of the kind studied by Hurst. Recently, Klemeš (1974) has surveyed the physical interpretations of the 'Hurst phenomenon' and expresses serious doubts about the usefulness of operational models for hydrological phenomena as suggested by Mandelbrot and his coworkers. Briefly, Klemeš argues that the assumption of stationarity over hundreds to thousands of years for geophyiscal time series is not reasonable, and constructs a stochastic process containing a zero span of dependence (zero memory) with a non-stationary mean which exhibits the Hurst phenomenon. Our purpose here is not to enter into the argument over the existence of stationarity in geophysical records but to point out a body of literature on the Hurst phenomenon and long-term persistence which has motivated the present study.

The first application of R/S analysis to turbulence was by Laushey (a discussant in Hurst 1951), who reported $H \approx 0{\cdot}65$ for velocity signals in the flow of water in a laboratory flume. Nordin *et al.* (1972) present evidence for the existence of the Hurst phenomenon in turbulent velocity records measured in laboratory flumes and in the Missouri and Mississippi Rivers. They show rescaled-range data for time periods of up to three decades which give Hurst coefficients of 0·60–0·84 for the flume measurements and 0·93–0·95 for the river measurements. None of their measurements of the rescaled range exhibits a break in the Hurst coefficient towards a state of asymptotic independence ($H = 0{\cdot}5$). Nordin *et al.* suggest that long-term persistence may arise from 'sporadic' turbulence caused by intermittency near the walls or boundaries or from vortex motions. Fischer (1973) believes that the Nordin *et al.* results can be explained by the existence of certain secondary flows. In their reply to Fischer, Nordin *et al.* (1973) agree that a secondary flow may explain their results, but they believe that such secondary flows are not a very common occurrence in river or channel flows.

Nordin *et al.* (1972) chose to study turbulence records primarily as a model for the Hurst phenomenon in geophysical time series, and they may well provide a suitable model for such a study. Our less ambitious objective here will be to discover what can be learned from an application of a rescaled-range analysis to grid turbulence, a well-studied canonical turbulent flow. It is known (see Frenkiel & Klebanoff 1967; Van Atta & Chen 1968) that the grid-turbulence velocity field is approximately Gaussian and that autocorrelations of the longitudinal and transverse velocity fluctuations decay to zero in about twenty grid time scales $\tau_g = M/U$, where M is the mesh size of the grid and U is the longitudinal mean velocity. Recalling that for a Gaussian process a constant integral of the autocorrelation implies independence, we expect to obtain Hurst coefficients approaching 0·5 for records longer than 20 τ_g. Preliminary rescaled-range calculations on some existing grid-turbulence data of Van Atta & Chen do exhibit regions with $H \approx 0{\cdot}5$, but there appears to be a break in the Hurst coefficient at large times, which motivated the taking of additional measurements appropriate for long-term rescaled-range calculations.

It is our purpose, then, to present evidence of a turbulence time series which does not exhibit the Hurst phenomenon for all times, but indeed exhibits two clearly distinct regions of the Hurst phenomenon separated by time scales giving $H \approx 0{\cdot}5$. We shall see that the Hurst region at small time lags is certainly a result of the 'long-term' persistence of the grid turbulence itself (when compared with τ_g), but that there is a region of independence followed by a break in the slope of the rescaled range at time scales which are characteristic of the wind-tunnel motions. Thus we shall argue that for grid turbulence there is a 'micrometeorology' separated from 'climatic' wind-tunnel motions because the two regions in which $H \neq 0{\cdot}5$ are separated by a region in which $H = 0{\cdot}5$, after a suggestion by Mandelbrot & Wallis (1969*b*). Finally we present some speculative arguments based on non-dimensionalized rescaled-range calculations of all the laboratory-flume, grid and river measurements.

2. Experimental conditions

Preliminary calculations of the rescaled range in grid turbulence used some data recorded on analog tape by Van Atta & Chen (1968). These data revealed some new and interesting features for the rescaled-range calculations, but it was clear that additional data were required to explore fully the implications of the early calculations. In particular, data of much longer duration were required to permit calculation of the rescaled range over a much wider range of time scales – time scales much larger than those normally used in the study of grid turbulence.

The measurements were made in the UCSD closed-circuit wind tunnel, which has a 76 cm × 76 cm × 10 m test section. A biplanar grid with a square mesh (mesh size $M = 2{\cdot}54$ cm) and cylindrical rods (0·477 cm in diameter) was located two tunnel diameters downstream from the entrance to the test section. The tunnel was operated at a mean speed of 15·7 m/s, which gave a grid Reynolds number of 27000. The mean velocity U and the velocity fluctuations u and v in the longitudinal and transverse directions were measured at a downstream location of $X/M = 48$. Additional experimental runs were made with the grid removed to investigate the properties of the wind tunnel alone.

The fluctuating velocities were measured with an X-wire array (DISA 55A38). The sensors were operated in the constant-temperature mode using DISA Model 55M01 hot-wire anemometer systems and were linearized with DISA Model 55D10 linearizers. Sum and difference amplifiers were used to obtain voltage signals proportional to u and v. The velocity fluctuations ($\langle u^2\rangle^{\frac{1}{2}} \approx \langle v^2\rangle^{\frac{1}{2}} \approx 30$ cm/s) were recorded on a Sangamo 3500 FM tape recorded at speeds of 60 and 7·5 in./s. The durations of the recording times at the two speeds were 5 min and 2·5 h respectively. The analog data were played back and digitally recorded by the AMES digitizer at various sample rates ranging from 66728 to 32·58 samples/s with 12-bit resolution. Each digital record (ensemble) contained 8192 velocity samples and each file (an aggregate of records) contained from 30 to 50 records to permit ensemble averaging of the rescaled range. The digital signals were analysed on the CDC 3600 computer at UCSD.

3. Data analysis

Rescaled-range calculations for the previously recorded grid-turbulence signals of Van Atta & Chen (1968) demonstrated the need for records covering very long time intervals in order to determine the extent of the asymptotic behaviour of R/S with the turbulence-generating grid in the wind tunnel. The preliminary results suggested that records covering long times could be constructed by keeping the number N of samples in a record constant and merely reducing the sample rate $SR = 1/\Delta t$, where Δt is the time between samples, to obtain sufficiently large times $T = N\Delta t$ for each record. The CDC 3600 at UCSD has a core size of 32000 words, so that a record containing about 8192 samples (powers of 2 are convenient for spectral analysis) is the largest which may be processed economically at one time. The digitizer used discards data samples during the writing of record gaps, causing severe upper limits on the time T for a record. Some digital acquisition systems preserve the continuity of the sampled data across the record gaps, but even with continuous data a serious problem remains. If the sample rate is held constant as the length T of the record is increased, the amount of computing required increases enormously. An alternative approach is to examine subintervals of the time interval desired with N held constant and to increase T by decreasing the sample rate.

Figure 1 shows results for a portion of the same turbulence signal processed with various sample rates. The calculations in figure 1(a) were performed by decimating the original digital time series and calculating the statistics for the rescaled range R/S. The same turbulence signal was used for each curve, and only the sample rate was changed. The most noticeable effect of varying the sample rate by two decades is an upward shift in the magnitude of the rescaled range with decreasing sample rate, but more important, there does not appear to be a change in the slope at constant T. In order to check this result more closely, the slopes from figure 1(a), shown in figure 1(b), were calculated using the first difference: $H = \ln\{(R/S)_{i+1}(R/S)_i^{-1}\}/\ln\{T_{i+1}T_i^{-1}\}$. There is considerable scatter in H, but there appears to be no consistent dependence of the slope on the sample rate. It is important to point out this result for, unfortunately, we earlier misinterpreted the data and concluded that there was sample-rate dependence. We are grateful to B. Mandelbrot for pointing out this error. In a review of an earlier draft of this paper, Mandelbrot demonstrated that the shift in the rescaled-range data with sample rate in figure 1(a) is due to our use of the Δt in the discretized version of the definition of R/S in (1)–(3). We have chosen to retain the Δt in our definition of R/S for purposes of scaling, but its presence is not required for estimation of Hurst coefficients. The independence from sample-rate effects implies that measurements of the rescaled range over many decades of time are both easy and economical, and do not require careful low-pass filtering of the signals as we initially concluded.

Feller (1951) shows that a theoretical estimate for the variance of the rescaled range is given approximately by

$$\operatorname{var}(R/S) \approx 0{\cdot}048(R/S)^2 \tag{4}$$

when R/S is asymptotic to $T^{\frac{1}{2}}$. This result can be used to estimate theoretically the variance of the ensemble-averaged rescaled range if one assumes that the M members of the ensemble are uncorrelated:

$$\operatorname{var}(\langle R/S\rangle) \approx 0{\cdot}048M^{-1}\langle R/S\rangle^2, \tag{5}$$

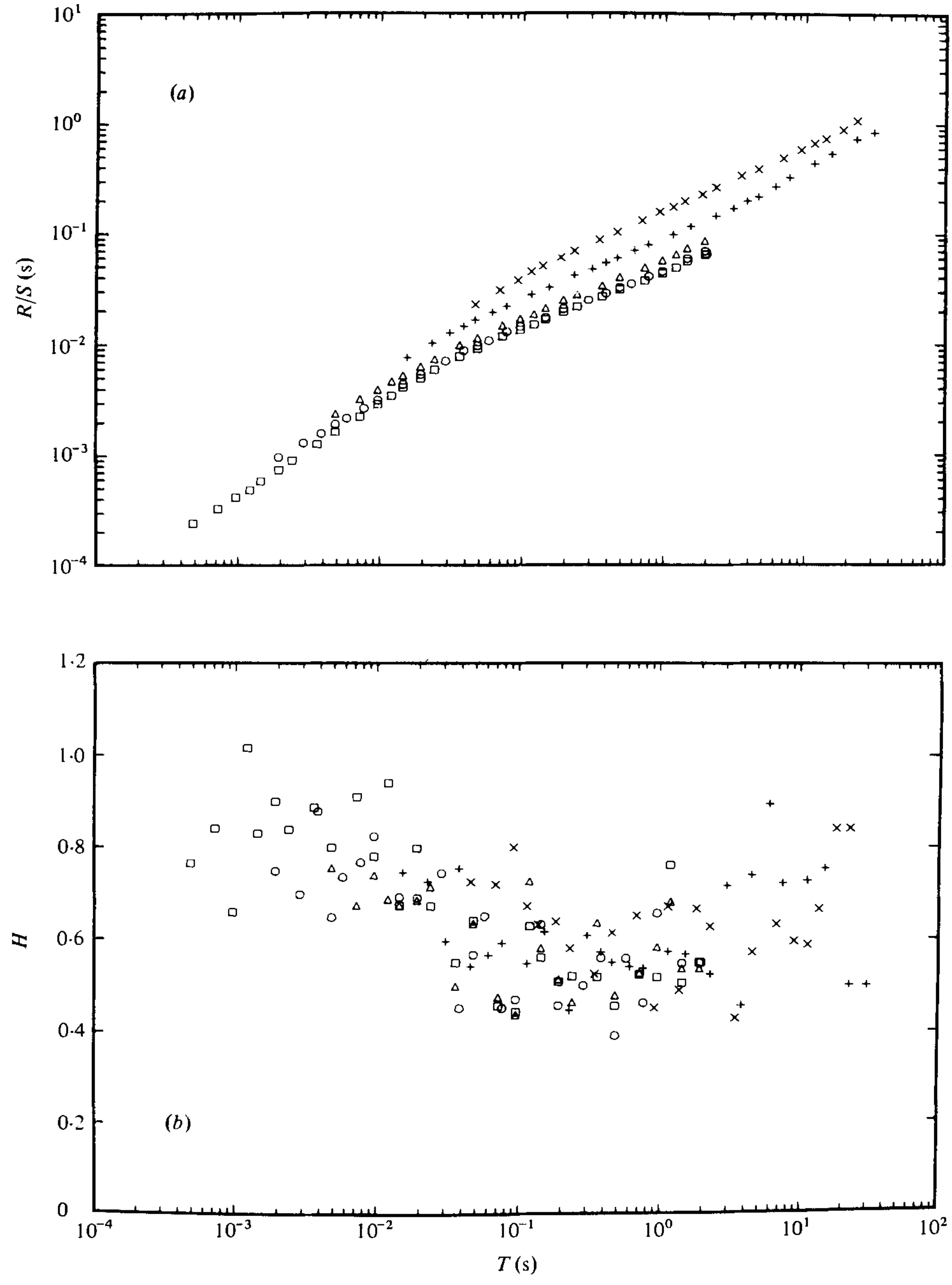

FIGURE 1. Examination of rescaled range and Hurst coefficient for sample-rate dependence. (a) Rescaled range R/S. (b) Hurst coefficient H. Sample rates: □, 4170 Hz; ○, 1042 Hz; △, 417 Hz; +, 130·5 Hz; ×, 43·5 Hz.

where the angle brackets denote ensemble averaging and M is the number of ensembles or records. The variance of $\langle R/S \rangle$ can also be directly estimated from the computations as

$$\operatorname{var}(\langle R/S \rangle) = M^{-2} \sum_{i=1}^{M} [(R/S)_i - \langle R/S \rangle]^2. \tag{6}$$

The ensemble-averaged rescaled range is given by

$$\langle R/S\rangle = M^{-1}\sum_{i=1}^{M}(R/S)_i. \tag{7}$$

Our data show that the theoretically predicted variance given by (5) compares favourably with the variance estimated directly from (6). Thus (5) provides a useful relation for estimating the number of records which are required for a given error. In the results presented herein, the number M of records was 50 for the higher sample rates and 30 for the lowest sample rate. If we take the ratio of the standard deviation of $\langle R/S\rangle$ to the estimate of $\langle R/S\rangle$ as a measure of the error or resolvability, then the relation

$$\mathrm{var}^{\frac{1}{2}}\left(\langle R/S\rangle\right)/\langle R/S\rangle \approx 0\cdot 22\, M^{-\frac{1}{2}} \tag{8}$$

can be used to estimate the approximate error we may expect in measurements of the rescaled range. For our case, this ratio is less than 4 %, which is in good agreement with the direct estimates of $\mathrm{var}^{\frac{1}{2}}(\langle R/S\rangle)/\langle R/S\rangle$ using (6) and the measurements. In the remainder of the paper the angle brackets denoting the ensemble-averaged R/S are dropped, ensemble averaging being understood.

4. Results

The rescaled ranges R/S for the u and v velocity components are presented in figure 2 on composite diagrams for four sample rates covering nearly seven decades of time. The good agreement among the slopes of the overlapping curves provides confidence in the data analysis techniques. There are some initial transients in the first decade for the two lowest sample rates (largest times), but both sets of points merge into a single curve at large times. The results reported herein come from a single experimental run, but additional runs had nearly identical behaviour and are thus not presented.

There is an initial steep slope in R/S extending over three decades for both the u and the v component in figure 2. The slope is always close to 1·0 for small T, then monotonically decreases towards $\frac{1}{2}$ for intermediate values of T. Slopes near $H = 1\cdot 0$ require closer examination, possibly along the lines of Mandelbrot (1975). The u component appears to contain about a decade where $R/S \sim T^{0\cdot 5}$ followed by a second break after which R/S rises sharply, approaching a slope of 0·78. There is no indication that further breaks in the trend beyond $T = 10$ s might be observed. The R/S for the v component exhibits a break in the steep initial trend about half a decade before that for the u component, but there does not appear to be any region where $H \approx 0\cdot 5$ like that seen for the u component. There is a second break in R/S towards a slope of 0·68 for the v component, likewise occurring about half a decade before the similar break for the u component. The Hurst coefficients for each time interval are summarized in table 1 for both the u and the v component.

The approach of R/S to the theoretical Hurst coefficient for independence ($H = 0\cdot 5$) can be examined more closely by presenting the R/S data multiplied by $T^{-0\cdot 5}$ on semi-logarithmic scales. Logarithmic scales are notorious for masking small differences, and if R/S has a $T^{0\cdot 5}$ behaviour, it will appear as a region where $R/(ST^{0\cdot 5}) =$ constant in the modified presentation. This technique has been applied to R/S for the

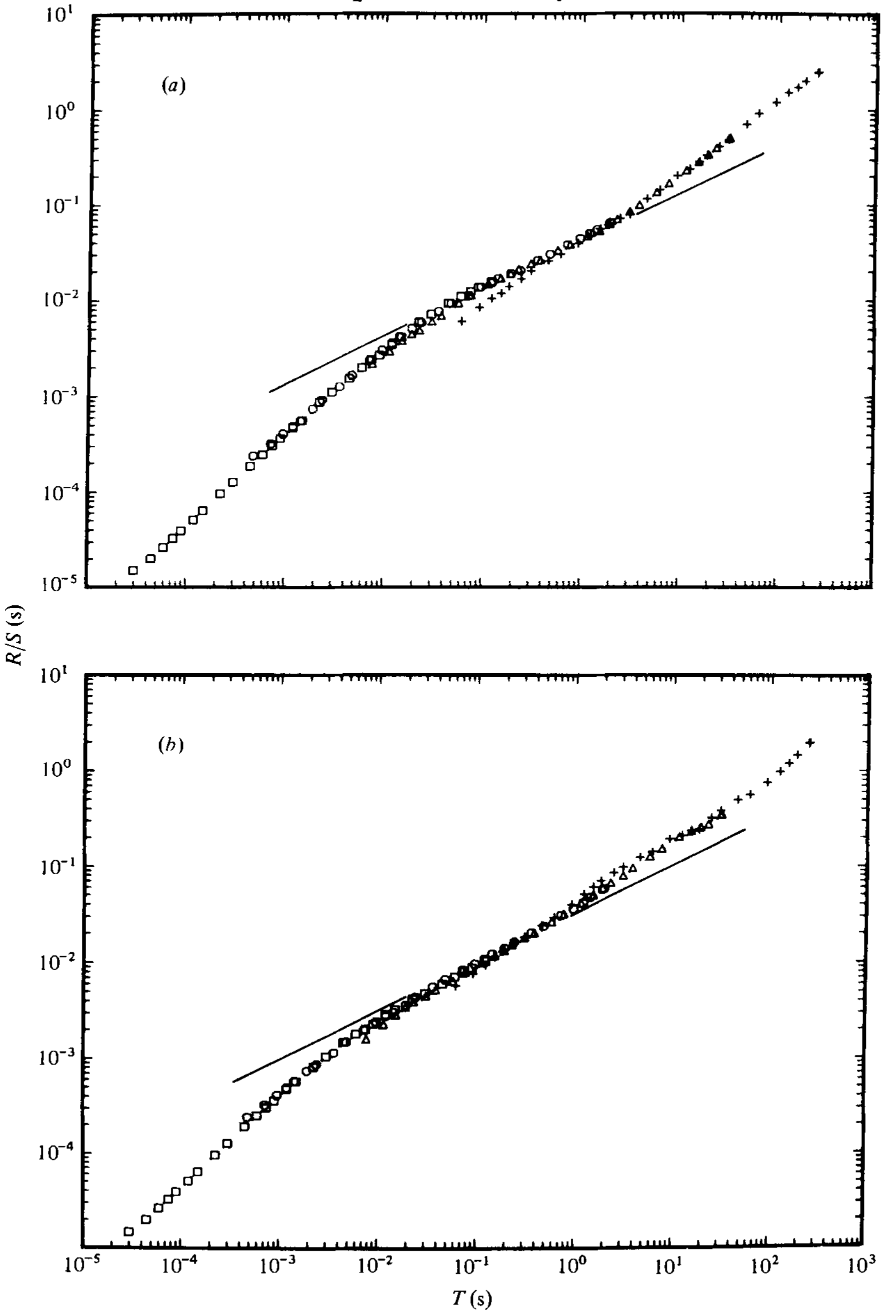

FIGURE 2. Rescaled range $R(t, T)/S(t, T)$ for grid turbulence. (a) u component. (b) v component. Sample rates: □, 66728 Hz; ○, 4170 Hz; △, 260·6 Hz, 32·6 Hz. Solid lines have slopes of 0·5.

u and v components in figure 3. The u component clearly exhibits somewhat more than a decade where $R/S \sim T^{0.5}$, but the v component does not approach a slope $H = 0.5$ as closely. Some possible explanations for the observed difference between the u and the v components will be discussed in §5.

The power spectra for u and v are shown in figure 4. Mandelbrot & Wallis (1969a)

Data	Figure	Time interval (s)	H
u, grid in	2 (a)	$10^{-5} < T < 10^{-2}$	0·99
		$7 \times 10^{-2} < T < 3$	0·50
		$3 < T < 10^{2}$	0·78
v, grid in	2 (b)	$10^{-5} < T < 3 \times 10^{-3}$	0·98
		$10^{-2} < T < 1$	0·57
		$1 < T < 10^{2}$	0·68
u, grid out	6 (a)	$10^{-3} < T < 10^{2}$	0·95
v, grid out	6 (b)	$10^{-3} < T < 10^{2}$	0·93

TABLE 1. Hurst coefficients for grid turbulence at various time lags.

have related the spectrum of fractional Gaussian noise to the slope of the rescaled range by the expression

$$\phi \sim f^{1-2H}, \tag{9}$$

where ϕ is the power spectrum and f is the frequency. The spectra were computed using standard fast Fourier algorithms from the same data as were used to calculate the rescaled range. Each spectrum is a composite of results for five sample rates (two of which are identical but arise from different combinations of analog and digital recording speeds), and the low-pass-filter effects appear as an early cut-off in the spectral levels at frequencies of about 10 and 100 Hz. There appears to be reasonable agreement between the extent of the $R/S \sim T^{0\cdot5}$ region for the u component and the region where $\phi \approx$ constant for the power spectrum. In addition there is excellent agreement between time and frequency, according to the reciprocal relationship $T = 1/f$, throughout the $R/S \sim T^{0\cdot5}$ range. The relationship for the fractional Gaussian noise spectrum in terms of the Hurst slope might work fairly well over the low and intermediate frequency bands, but at the high frequencies we cannot expect the relationship to hold. Turbulence cannot be represented by fractional Gaussian noise for all frequencies, since as the frequency increases, the slope H of the R/S calculations is limited to $H \leqslant 1$ but the turbulent spectrum ϕ falls off much faster than the predicted f^{-1} for large f owing to viscous diffusion. The fractional Gaussian noise process or its relatives (the broken-line process, Nordin *et al.* 1972) can thus be used to construct operational models of turbulent processes over only part of the range of frequencies or scale sizes. The results for the v spectrum are similar. The v spectrum appears to have a small region where $\phi \approx$ constant, but it is clear from the plot of $R/(ST^{0\cdot5})$ for v in figure 3(b) that $H \neq 0\cdot5$ for any finite time interval. The criterion $H = 0\cdot5$ for the slope of the rescaled range appears to be somewhat more sensitive than the equivalent criterion $\phi =$ constant for the fractional Gaussian noise as a measure of dependence, and the rescaled-range test does not require an assumption of Gaussianity.

It is interesting to compare the time scales at which the u and v autocorrelations become zero with the time when H first attains a value near 0·5 in figure 3. The u and v correlations are presented in figure 5 in semi-logarithmic co-ordinates to show the approach to zero correlation. For a Gaussian process, a constant integral of the autocorrelation implies independence. The u correlation becomes zero for $T > 0\cdot03$ s ($UT/M > 18$) and the v correlation is zero for $T > 0\cdot01$ s ($UT/M > 6$), which implies a constant integral. The autocorrelations remain indistinguishable from

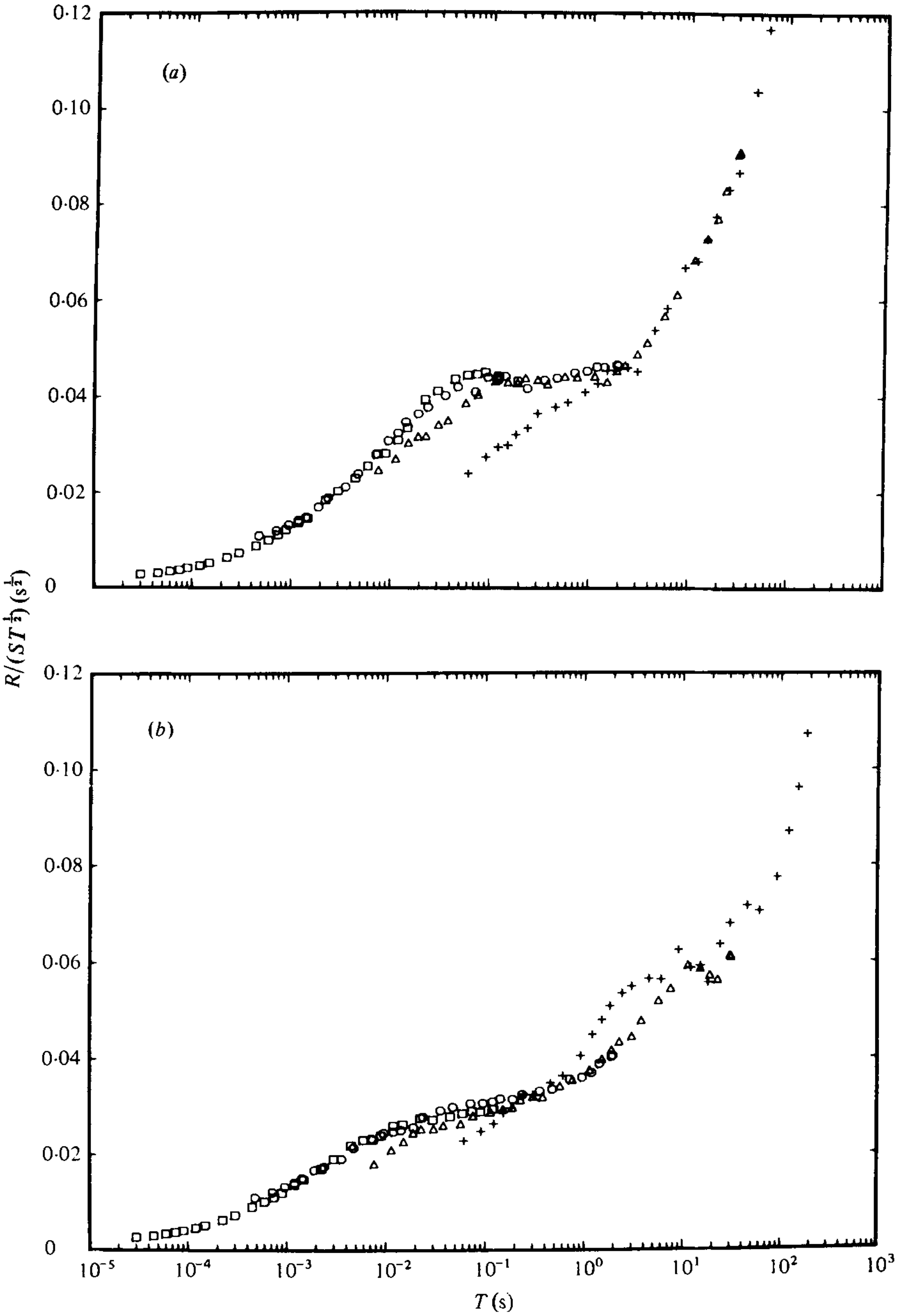

FIGURE 3. Rescaled range plotted to emphasize $R/S \sim T^{0.5}$ behaviour. (*a*) *u* component. (*b*) *v* component. See figure 2 for symbol definitions.

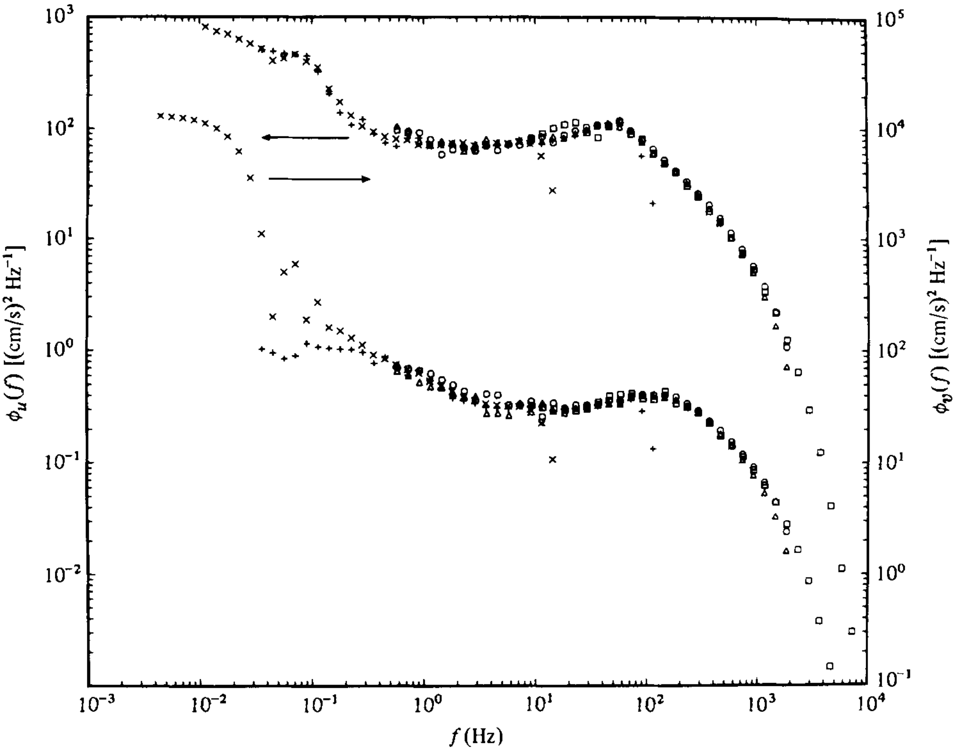

FIGURE 4. Power spectra of the u and v velocity components of grid turbulence. Sample rates: □, 66728 Hz; ○, 4170 Hz; △, 4170 Hz ; +, 260·6 Hz; ×, 32·6 Hz.

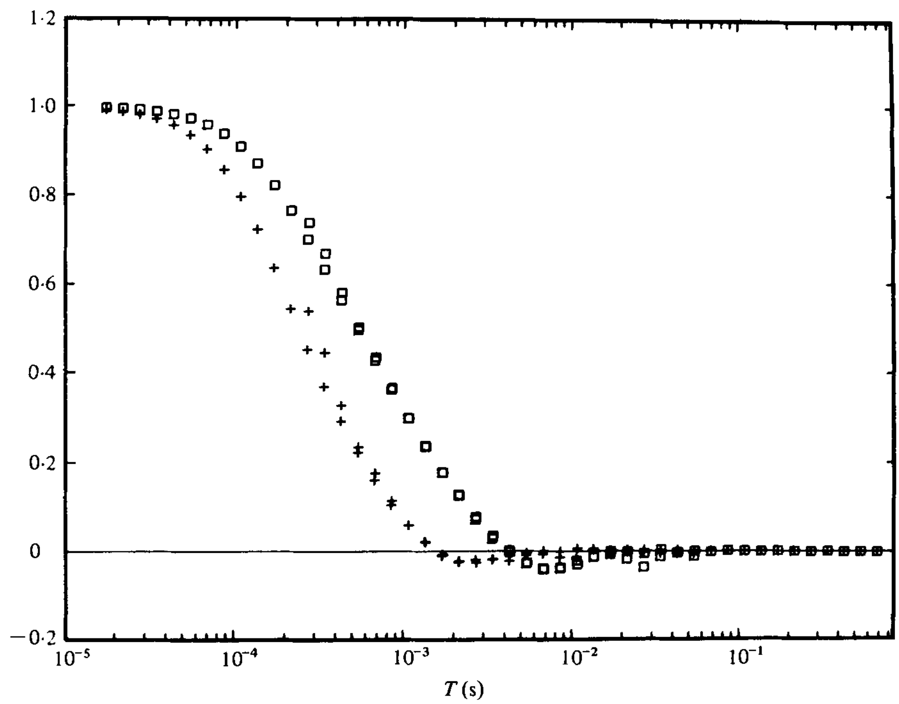

FIGURE 5. Autocorrelations for grid turbulence. □, $\langle u(t+T)\, u(t)\rangle/\langle u^2\rangle$; +, $\langle v(t+T)\, v(t)\rangle/\langle v^2\rangle$.

zero for time lags up to 250 s (not shown in figure 5). These correlations are nearly identical to those reported by Van Atta & Chen (1968, 1969). From table 1, H approaches 0·5 at times T of 0·07 and 0·01 s for the u and the v components respectively. The difference between the rescaled-range and autocorrelation estimates for independence are probably within the measurement errors. While both the rescaled-range analysis and the correlation analysis with an assumption of Gaussianity appear to imply independence at nearly the same time lag, this is apparently not true for larger times. As observed in figure 3, the rescaled ranges of u and v break from $H = 0{\cdot}5$ and rise with significantly steeper slopes, but the autocorrelations remain zero. We suspect that the rescaled range may be a more sensitive measure of residual dependence than the autocorrelation and, importantly, it does not require a Gaussian assumption. It should also be noted that while the integral of the v autocorrelation does approach a constant for $T > 0{\cdot}01$ s, the Hurst coefficient for the v component remains significantly above 0·5 in the same time interval.

In order to obtain more information on the interaction of grid turbulence with the wind-tunnel motions, measurements were made with the velocity sensors in the same position but with the grid removed. The results for the u and v components are shown in figure 6. The rescaled range for both the u and the v signal rises at nearly constant slope with only minor fluctuations. There are no breaks in the Hurst coefficients like those observed in the measurements made with the grid. The Hurst coefficients for the runs with the grid removed are compared with the grid runs in table 1.

5. Discussion

A very simple explanation for the behaviour of the Hurst coefficient in the wind tunnel is possible. With the grid removed from the wind tunnel, the relatively low frequency velocity fluctuations caused by various phenomena such as eddy motions from the fan blades, residual turbulence generated in the boundary layers, acoustic waves and influences of the room (the wind tunnel is closed, but is not pressure sealed from the room) produce a spectrum which falls off with increasing frequency. When the grid is introduced additional velocity fluctuations are superimposed on the background turbulence level, mostly at the higher frequencies. If one supposes that the fractional Gaussian process provides at least a crude operational model for the turbulence, then the rescaled range will attain a Hurst coefficient of 0·5 only where the falling background spectrum is just balanced by the rising grid-generated spectrum. Since turbulent velocity fluctuations can often be approximated by a Gaussian probability density function, a prediction based on spectral measurements should provide a good estimate for the behaviour of the Hurst coefficient for a wide variety of turbulent flows.

Mandelbrot & Wallis (1969*b*) suggest that in order to make a meaningful distinction between disciplines such as meteorology and climatology the rescaled-range analysis of the time series should exhibit a region where $R/S \sim T^{0{\cdot}5}$ between the time scales associated with phenomena described by each discipline. If this condition is met, it is then useful to speak of a 'meteorology' independent of the climatic time scales, which greatly simplifies the practical problem of analysis and model building. If the region of independence can be shown to exist, it should be possible to construct

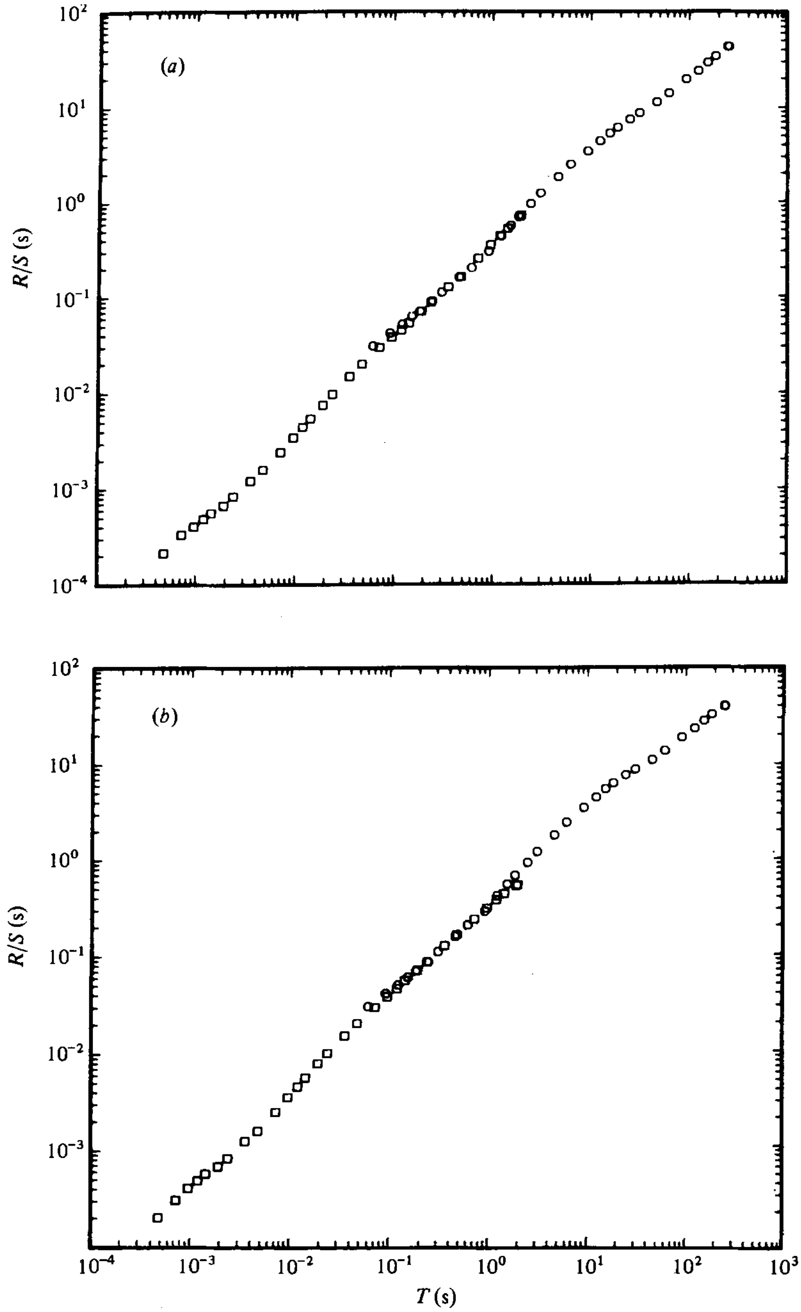

FIGURE 6. Rescaled range of the wind-tunnel flow with the grid removed. (a) u component. (b) v component. Sample rates: □, 4170 Hz; ○, 32·6 Hz.

models for each region of scales separately. Figure 3 shows that the u velocity fluctuations with time scales less than 0·1 s are independent of velocity fluctuations on time scales larger than 3 s. For times larger than 3 s the wind tunnel dominates the fluid motions, and it would be pointless to include these fluctuations in a comparison with, say, an idealized model of isotropic grid turbulence.

The power spectra presented in figure 4 illustrate the danger in extrapolating to 'zero' frequency to obtain an estimate of the integral scale of turbulence. Usually one does not take sufficient data to resolve frequencies much below 1 Hz in wind-tunnel experiments, and there are serious problems in defining a finite integral scale in this manner. Comte-Bellot & Corrsin (1971) have discussed the estimation of integral scales in grid turbulence. Briefly, they show that it is impossible, in principle, to measure the integral scale (since infinite times are required), and even if this were possible the resulting integral scale would have no meaning for the grid-turbulence experiment. As the frequency is reduced, the scales become larger until eventually fluid motions with dimensions of the order of the wind-tunnel size dominate the spectrum. Instead, they suggest extrapolating the 'real' flow to some hypothetically possible flow, with the two merging at some frequency. The R/S analysis provides quantitative information which can be used to judge the frequency or time scale where the size of the experimental apparatus becomes important. The R/S subrange with $H \sim 0{\cdot}5$ which exists in the u component and to a lesser extent in the v component of the present measurements implies that models of the grid-turbulence flow could be compared with data with time scales less than 1·0 s without incorporating information about the wind-tunnel dimensions into the model estimates. The argument for the v component measured in the present study is weaker, since H deviates somewhat from 0·5. We suspect that for practical purposes an H of 0·57 may indicate a sufficient degree of independence so that v can be considered to have a time scale below which the turbulence is approximately independent of the large-scale wind-tunnel circulations. The rescaled range can provide an objective method for defining the lowest frequencies which are not dominated by fluid motions on the scale of the wind tunnel.

The runs with the grid removed are similar to the laboratory measurements of Nordin *et al.* (1972) in a flume as well as their measurements in the Mississippi and Missouri Rivers. Without the grid, the wind-tunnel flow is similar to the open-channel flows in the flume and rivers; the grid superimposes an additional set of fluid motions. There is an important difference, however, for the wind tunnel was run closed with a transit time of about 12 s. This would seem to guarantee a long-term persistence on time scales greater than 12 s. It might be interesting to repeat these measurements with the tunnel run open, thus preventing any very obvious dependent mechanisms. However, we suspect that no difference would be observed, since the rescaled range for the runs without the grid has a nearly constant Hurst coefficient for time scales much smaller than the 12 s tunnel transit time. The large H observed for the runs with the grid removed may be evidence for a kind of secondary flow at very low frequencies similar to that suggested by Fischer (1973) to explain the large Hurst coefficient in the laboratory-flume measurements. The observed behaviour of R/S for the wind tunnel may be due to closed-loop effects or unsteady fan-blade response which is smoothed out by the diffuser, the turns, and many layers of screening in the settling chamber.

Finally we suggest a possible explanation for the differences between the forms of R/S for the u and v velocity components. The first break in the slope of R/S for v occurs before the first break in the slope for u. This is probably a feature of grid turbulence, for the spectrum of v crosses over the spectrum of the u component at a frequency of about 100 Hz (note that different scales are used for the u and

v spectra in figure 4) and remains above as the frequency increases. It is well known (Batchelor 1953, p. 48) that the transverse autocorrelation decays to zero (first zero crossing) well before the autocorrelation for the u component. This comparative behaviour is similar to that of low-pass-filtered white noise. As the bandwidth increases, the autocorrelation goes to zero faster, the limiting case of a pure white-noise spectrum corresponding to a delta function for the corresponding autocorrelation. The R/S of the v component does not approach $H \sim 0{\cdot}5$ as closely as that of the u component. The aspect ratio of the wind tunnel may be partially responsible for this difference. The wind tunnel has a length-to-width aspect ratio of about 30, and it is likely that this large aspect ratio is in some way responsible for the different rescaled-range slopes for the u and v components at large times.

6. Non-dimensional scaling

For geometrically similar flows, dimensional analysis suggests the conclusion that the non-dimensionalized rescaled range, i.e. the product of R/S and the reciprocal of the characteristic time scale, may be a function only of the dimensionless time, which is T divided by a characteristic time scale. This choice of scaling is not unique and may prove to be controversial. We have normalized R/S data for hydrological river-level records, river and velocity fluctuations, laboratory-flume experiments and grid experiments (the 7·7 and 15·7 m/s data of Van Atta & Chen (1968) therein referred to as low- and high-speed grid data), using characteristic times appropriate for each situation. For the grid flow, the characteristic correlation time scale is known to be well represented by M/U. For the river velocity fluctuations measured by Nordin *et al.* (1972) we have chosen U as the mean river velocity and M as the depth. For the annual Nilometer readings of Hurst (1951), we have used a characteristic time scale of ten years. The latter is probably too small and is the most uncertain figure of all, but we shall see that an error of even an order of magnitude will not affect our conclusions. As shown in figure 7, this scaling results in a remarkable collapse of all the data towards a single dimensionless curve extending over a range of nearly 10^9 in UT/M and 10^8 in RU/SM. For the smaller values of UT/M the curve displays a Hurst-phenomenon type of behaviour, with a slope of about 1·0. For larger values of UT/M, the slope decreases until a range is reached in which the slope is about $\frac{1}{2}$, but for still larger values of UT/M the slope of the curve again increases. The region of approximate validity of the theoretical relation $R/S \sim T^{0 \cdot 5}$ spans only slightly more than one decade of UT/M, roughly $10^2 \leqslant UT/M \leqslant 10^3$. Only the data for the small flume, the low-speed grid and the high-speed grid were recorded for sufficiently long times to span this interval. The Nile data end at an upper limit of $UT/M = 104$, the Missouri data at $UT/M = 47$ and the Mississippi data at $UT/M = 15$. Only the grid and small flume data cover a sufficiently large range to exhibit all three regions of behaviour in a single time series.

The scaled data suggest the possibility that the river data might have shown a break from the behaviour associated with the Hurst phenomenon if records extending for a factor of 10–10^2 longer could have been obtained. Nile records extending back in time through the most recent ice age would be necessary to satisfy this requirement.

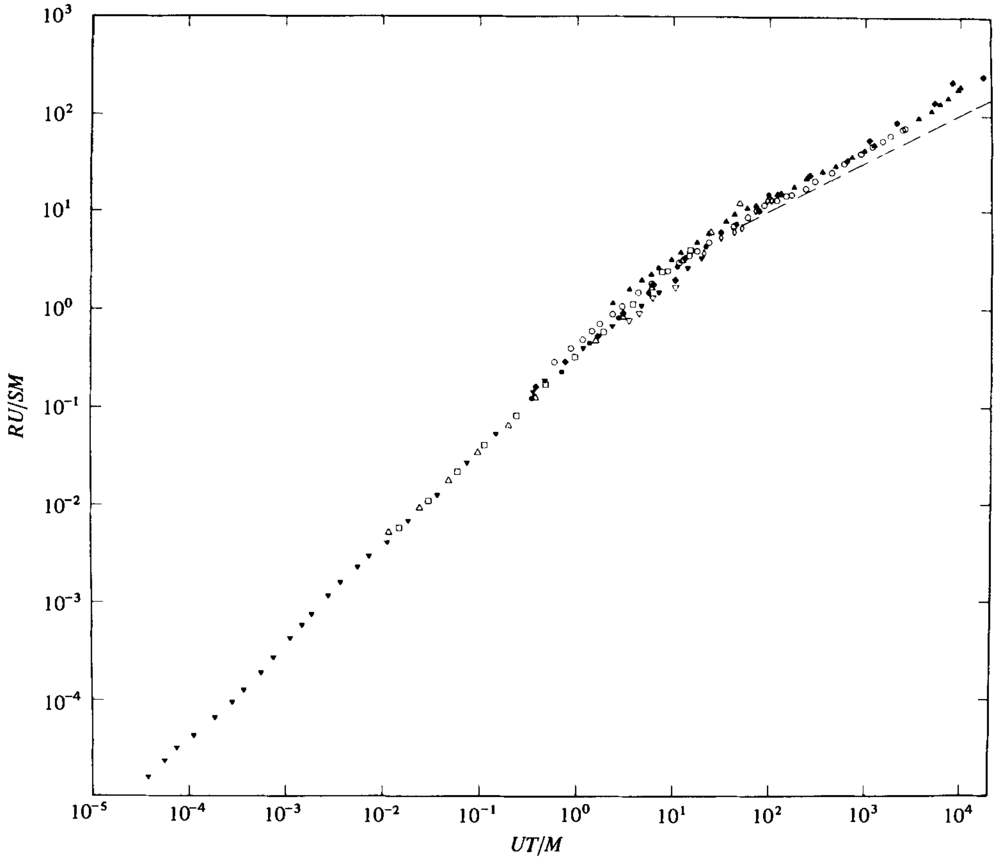

FIGURE 7. Non-dimensional rescaled range for various time series. ◇, Nile; □, Mississippi; △, Missouri; ▽, river levels, discharges and run-off; ◆, 8 in. flume; ●, 4ft flume; ○, low-speed grid; ▲, high-speed grid; ▼, grid removed. Dashed line has slope 0·5.

Future Nile records, even very long ones, may not be useful in extending the older data because of basic changes in hydrological parameters due to extensive engineering work in this century. It should be possible, however, to obtain suitable longer records for turbulent fluctuations in rivers and in laboratory flumes, for which the characteristic time scales of the fluctuations of interest are much shorter.

7. Summary

The theoretically predicted asymptotic slope $H = 0{\cdot}5$ has been found for the rescaled range for nearly a decade of time intervals for the u component of a grid-generated turbulent velocity field. The v component approaches a slope $H = 0{\cdot}57$ in the present study. The differences observed between the R/S curves for the u and v components may be in part a result of the large wind-tunnel length-to-width aspect ratio (about 30:1). The initial slopes for the u and v components both approach within a few per cent of $H = 1$, corresponding to strong dependence for time separations less than about 0·07 s. This is consistent with previous measurements of grid turbulence and corresponds to the regions of finite u and v autocorrelations.

While grid turbulence has been emphasized in the present study, questions of long-term dependence are important for any laboratory turbulence investigation. The experimenter seeks measurements which are independent of certain large-scale features of the experimental apparatus. In the present study, we see that the grid-generated turbulence is quantitatively separable from the properties of the wind tunnel itself. The high frequencies ($f > 0{\cdot}5$ Hz) are dependent not on the gross features of the wind tunnel but primarily on the generating grid of rods. The methods used in the present study to examine the dependence of grid turbulence on the gross features of the wind-tunnel characteristics should be applicable to other laboratory situations. For example, in the study of a free jet issuing into a room of finite dimensions one would like to know quantitatively the lowest frequencies which are directly dependent on features of the jet turbulence and not dominated by the room itself. The rescaled range may prove to be a useful tool in quantifying the boundary between the turbulent signal and the background noise.

The authors thank Mr R. A. Stanford for helpful suggestions which greatly increased the speed of the computer code. In addition, the authors thank the referees for their helpful comments and criticisms. This work has been supported by National Science Foundation Grant ENG76-13147 and by the Office of Naval Research, under Contract N00014-76-C-0702.

REFERENCES

ANIS, A. A. & LLOYD, E. H. 1953 On the range of partial sums of a finite number of independent normal variates. *Biometrika* **40**, 35.

BATCHELOR, G. K. 1953 *The Theory of Homogeneous Turbulence.* Cambridge University Press.

COMTE-BELLOT, G. & CORRSIN, S. 1971 Simple Eulerian time correlation of full- and narrow-band velocity signals in grid-generated, 'isotropic' turbulence. *J. Fluid Mech.* **48**, 273.

FELLER, W. 1951 The asymptotic distribution of the range of sums of independent random variables. *Ann. Math. Statist.* **22**, 427.

FISCHER, H. B. 1973 A possible explanation for Nordin, McQuivey and Mejia's observation of the Hurst phenomenon in turbulence. *Water Resources Res.* **9**, 492.

FRENKIEL, F. N. & KLEBANOFF, P. S. 1967 Higher-order correlations in a turbulent field. *Phys. Fluids*, **10**, 507.

HURST, H. E. 1951 Long-term storage capacity of reservoirs. *Trans. A.S.C.E.* **116**, 770.

KLEMEŠ, V. 1974 The Hurst phenomenon: a puzzle? *Water Resources Res.* **10**, 675.

LLOYD, E. H. 1967 Stochastic reservoir theory. *Adv. in Hydrosci.* **4**, 281.

MANDELBROT, B. B. 1965 Une classe de procèssus stochastiques homothétiques à sui; application à la loi climatologique de H. E. Hurst. *C. R. Acad. Sci. Paris* **260**, 3274.

MANDELBROT, B. B. 1975 Limit theorems on the self-normalized range for weakly and strongly dependent processes. *Z. Wahrscheinlichkeitstheorie verw. Gebiete* **31**, 271.

MANDELBROT, B. B. & VAN NESS, J. W. 1968 Fractional Brownian motions, fractional noises and applications. *S.I.A.M. Rev.* **4**, 422.

MANDELBROT, B. B. & WALLIS, J. R. 1969*a* Computer experiments with fractional Gaussian noises. 1, Averages and variances; 2, Rescaled ranges and spectra; 3, Mathematical appendix. *Water Resources Res.* **5**, 228.

MANDELBROT, B. B. & WALLIS, J. R. 1969*b* Some long-run properties of geophysical records. *Water Resources Res.* **5**, 321.

NORDIN, C. F., MCQUIVEY, R. S. & MEJIA, J. M. 1972 Hurst phenomenon in turbulence. *Water Resources Res.* **8**, 1480.

NORDIN, C. F., MCQUIVEY, R. S. & MEJIA, J. M. 1973 Reply. *Water Resources Res.* **9**, 494.

VAN ATTA, C. W. & CHEN, W. Y. 1968 Correlation measurements in grid turbulence using digital harmonic analysis. *J. Fluid Mech.* **34**, 497.

VAN ATTA, C. W. & CHEN, W. Y. 1969 Correlation measurements in turbulence using digital Fourier analysis. *Phys. Fluids Suppl.* **12**, II 264.